Supporting Information

miRNA sensing hydrogels capable of self-signal amplification for early diagnosis of Alzheimer's disease

*Jaewoo Lim[1,2], Sujin Kim[3], Seung Jae Oh[4], Song Mi Han[5,6,7], So Young Moon[6], Byunghoon Kang[1], Seung Beom Seo[1,8], Soojin Jang[1,2], Seong Uk Son[1,2], Juyeon Jung[1,2], Taejoon Kang[1], Sun Ah Park[5,6,7], Minho Moon[3,] *, Eun-Kyung Lim[1,2,] **

[1] Bionanotechnology Research Center, Korea research institute of bioscience and biotechnology (KRIBB), 125 Gwahak-ro, Yuseong-gu, Daejeon, 34141, Republic of Korea.

[2] Department of Nanobiotechnology, KRIBB School of Biotechnology, University of Science and Technology, 125 Gwahak-ro, Yuseong-gu, Daejeon, 34113, Republic of Korea.

[3] Department of Biochemistry, College of Medicine, Konyang University, 158, Gwanjeodong-ro, Seo-gu, Daejeon 35365, Republic of Korea.

[4] YUHS-KRIBB Medical Convergence Research Institute, College of Medicine, Yonsei University, 50 Yonsei-ro, Seodaemun-gu, Seoul 03722

[5] Department of Cogno-Mechatronics Engineering, Pusan National University, 2 Busandaehak-ro 63beon-gil, Geumjeong-gu, Busan 46241, Republic of Korea.

[6] Lab for Neurodegenerative Dementia, Department of Anatomy, Ajou University School of Medicine, 164 World Cup-ro, Yeongtong-gu, Suwon 16499, Republic of Korea.

[7] Department of Neurology, Ajou University School of Medicine, 164 World Cup-ro, Yeongtong-gu, Suwon 16499, Republic of Korea.

[8] Neuroscience Graduate Program, Department of Biomedical Sciences, Ajou University Graduate School of Medicine, 164 World Cup-ro, Yeongtong-gu, Suwon 16499, Republic of Korea.

2. Experimental sections

2.1. Reagents and materials

Poly(ethylene glycol) (Mn 3,350) (PEG 3.35K), *N,N*-diisopropylethylamine (DIPEA), dichloromethane (DCM), chloroform, L-α-phosphatidylcholine (PC), 3β-hydroxy-5-cholestene (Cholesterol), 2-hydroxy-2-methylpropiophenone (HMPP) as a radical photo-initiator, 1,2-dioleoyl-3-trimethylammonium-propane (DOTAP), Nile red, and Triton™ X-100 were purchased from Sigma-Aldrich (USA). Acryloyl chloride was purchased from Tokyo Chemical Industry Co (TCI, Japan). Buffers 10×TBE and 1×TE were purchased from Biosesang (Korea). Polydimethylsiloxane (PDMS) elastomer (Sylgard® 184) was purchased from Dow Corning. Acrylamide/Bis-acrylamide solution (19:1, 40%), tetramethylethylenediamine (TEMED), and ammonium persulfate (APS) were purchased from Bio-Rad Lab., Inc (USA). Ultra-low range DNA ladder was purchased from Thermo Fisher Scientific, Inc (USA). Amicon® ultra centrifugal filter (molecular weight cut-off: 50 K) was purchased from Merck Millipore (USA). ExoRNeasy Maxi kit, RNeasy Mini Kit, miScript II RT kit, and miScript SYBR Green PCR Kit were purchased from Qiagen (Germany).

2.2. Synthesis of CHA hairpins for AD-related biomarker detection

CHA hairpins were designed to amplify fluorescence signals through sequential self-cycling in non-enzymatic conditions for high-sensitive detection of AD-related biomarkers (T). These CHA hairpins consisted of two hairpin-structured probes (H1 and H2), with which T could be detected at high sensitivities through a non-enzymatic cascade reaction based on FRET.

To detect T via fluorescence, H1 was modified with fluorescein (FAM; Ex/Em, Max =492/518 nm) at the 5’ end, and BHQ1 at the 3’ end. Before the experiment, each probe was annealed at 90 °C for 5 min and cooled down slowly to room temperature for a hairpin structure formation. All hairpins were stored at −20 °C until use, such that the suppression of fluorescence signal

was well maintained. All hairpin sequences are listed in Table S1 and were purchased from Bioneer (Korea). First, we tested T detection using synthetic genes; DNA sequence was used instead of RNA sequence. The cascade reaction of CHA hairpins enabled fluorescence signal amplification, which was confirmed via polyacrylamide gel electrophoresis (PAGE) analysis. After the probes that serially reacted in each step were loaded onto the gel, the sample was run on a 10% acrylamide solution with 1 × TBE buffer under constant voltage (80 V) for 1.5 h at room temperature, and then stained with nucleic acid staining dye (Gel-Red) for 10 min to visually confirm the CHA reaction using a gel imaging system (Bio-Rad Laboratories, USA).

2.3. Preparation of bioprobe-containing lipoplex nanoparticles

To stably load hairpins without nonspecific reactions, each hairpin was individually loaded into lipoplex nanoparticles. First, lipoplex nanoparticles were prepared according to the classical thin lipid film hydration method (Zhang 2017). A total of 7 mg of PC, 0.7 mg of DOTAP, and 1.95 mg of cholesterol were dissolved in 10 mL of chloroform solution. The solution was evaporated using a rotary vacuum evaporator system at room temperature. Subsequently, 1 mL of 10 nM probe in TE buffer solution was added to the lipid film. The solution was then vortexed at maximum speed to ensure detachment of the lipid film from the glass wall of the recipient. For stability, the liposome was stored overnight at 4 °C. The lipoplex nanoparticle solution was centrifuged at 4,000 rpm for 1 h at 4 °C using an Amicon® ultra centrifugal filter to remove unloaded pre-probes. The obtained solution was stored at 4 °C until use.

2.4. Characterization of lipoplex nanoparticles

CHA-hairpin-loaded lipoplex nanoparticles were observed via fluorescence microscopy. Nile red (1 μg), a lipid staining dye, was added to the mixed lipid solution for visual confirmation of the degradation of H1-loaded lipoplex nanoparticles. cryo-SEM images were captured using

ZEISS crossbeam 550 (FIB-SEM). The samples were first mounted on a cryo-SEM sample holder, and then plunged into a freezing liquid ethane bath and then transferred to a liquid nitrogen bath. Once cooled down, both sample holder and specimen were transferred to a protected atmosphere shuttle under low temperature and vacuum conditions to prevent contamination. We then place them into the cryo-SEM sample preparation system to expose a fracture profile of the network, by impacting the cross section of the specimen with a blade. Finally, the specimen was transferred via the same shuttle to the pre-cooled SEM chamber to be imaged.

2.5. Preparation of lipoplex-composite hydrogel

First, polyethylene glycol diacrylate (PEGDA) was synthesized as a hydrogel backbone according to previously published protocols (Elbert and Hubbell 2001; Stevens et al. 2015). First, 60 g of PEG was completely dissolved in 75 mL of DCM. After the solution became transparent, 7 mL of DIPEA was injected, followed by dropwise injection of 6.5 mL acryloyl chloride while the mixture was stirred vigorously on ice, at 4 °C. This mixture was stirred overnight under a nitrogen atmosphere in the absence of light. Subsequently, this reactant was precipitated in 1 L of diethyl ether and filtered, and the filtrate was vacuum dried to obtain a powder. To eliminate by-products, the obtained powder was dissolved in 75 mL of DCM and 500 mL 2M potassium carbonate (K_2CO_3) to phase-separate the solution overnight. The lower organic solution was filtered and precipitated in 1 L of diethyl ether and dried under vacuum. Synthesized PEGDA was stored at 4 °C until further use. The lipoplex-composite hydrogels were prepared via photopolymerization of PEGDA. Aqueous solutions containing PEGDA (20 wt %), PEG (20 wt %), CHA-hairpin-loaded lipoplex (20 pmol of the probe), and 0.1 % (w/v) HMPP were poured into this mold and then photopolymerized using a UV lamp at a wavelength of 365 nm for 2 min. The fabricated lipoplex-composite hydrogels were rinsed in DW for 2 h

and dried overnight at room temperature. After the hydrogels were completely dry, they were also stored at 4 °C until further use.

2.6. Fabrication of hydrogel mold

The hydrogel mold was manufactured using a photo-curing 3D printer and bound onto a PDMS mold. The design of the hydrogel mold is shown in **Figure S1**. A mixture of base and curing agent (10:1 weight ratio) was poured into a cylinder- or cone-shaped hydrogel mold and heated at 80 °C for 6 h.

2.7. AD-related biomarker screening using 5XFAD mouse model

miRNA expressed in the 5XFAD mouse brain (hippocampus) and plasma was analyzed to select appropriate AD-related biomarkers. 5XFAD mice and their wild-type littermates were used in this study. A total of 14 mice were divided into 2 groups of 7 mice: (1) 5XFAD mice and (2) wild-type mice. Four-month-old female mice were used for all animal experiments. The 5XFAD mice (Tg6799 line) express five familial AD-related mutations in the human PSEN1 gene (M146 and L286) and APP gene [K670N/M671L (Swedish), V717I (London), and I716V(Florida)]. We purchased 5XFAD mice from the Jackson Laboratory (Bar Harbor, ME, USA). The transgenic mice were genotyped using polymerase chain reaction (PCR), and their wild-type littermates were used as a control. All mice were maintained at 20–25 °C, 45–55% humidity, and 12 h light/dark cycle, with free access to food and water. All protocols were reviewed and approved by the animal ethics committee of the University of Konyang. Animals were anesthetized via intraperitoneal injection of Avertin (Tribromoethanol; Sigma-Aldrich, St. Louis, MO, USA) at a dose of 250 μg/kg. Blood samples were collected from the mouse orbital sinus. To prevent blood clotting, we added 2 μl of heparin to the whole blood and centrifuged it at 13,000 rpm, at 4 °C for 15 min. The supernatant was immediately aliquoted,

and the samples were stored at −80°C. In addition, the brain was dissected into the hippocampus and frozen for subsequent RNA and protein extraction.

2.8. microRNA expression profiling using microarrays

Raw data were extracted automatically via the Affymetrix data extraction protocol using software provided by Affymetrix GeneChip® Command Console® Software (AGCC). The CEL files import, miRNA level RMA+DABG-All analysis, and result export were all performed using Affymetrix® Power Tools (APT) Software. Array data were filtered using probes annotated by species. Comparative analyses between test samples and control samples were conducted using fold change. For a significant DEmiRNA set, hierarchical cluster analysis was performed using complete linkage and Euclidean distance as a measure of similarity. All statistical tests and visualizations of differentially expressed genes were conducted using R statistical language 3.3.3 (https://www.r-project.org/).

2.9. RNA isolation and quantitative real-time PCR

The hippocampus, which is a part of the brain, was homogenized using a tissue grinder with a pestle in QIAzol lysis reagent, and total RNA was extracted using the miRNeasy kit (Qiagen) according to the manufacturer's protocol. Total RNA in blood was extracted using the exoRNeasy Maxi kit (Qiagen) according to the manufacturer's protocol. RNA quantity was determined using Nanodrop™ 2000 (Thermo Scientific), and equal amounts of each sample were used for first-strand cDNA synthesis using miScript II RT Kit (Qiagen). Quantitative PCR (qPCR) reactions were run on a CFX96™ Real-Time PCR System (Bio-Rad) according to the protocol of miScript SYBR Green PCR Kit. The expression levels of different miRNAs were estimated via normalization to U6.

2.10. Fluorescence measurement

The fluorescence intensities of the probes were observed with a fixed gain (λ_{ex} = 484 nm and λ_{em} = 530 nm) and measured on a Cytation 5 plate reader (BioTek). The increase in fluorescence intensities of probes before and after treatment with the target gene was measured. Concentrations of 2.5 pM for both probes (50 μL) were mixed, and the fluorescence intensity (F_0) was measured prior to treatment with the target gene. Afterward, 10 nM of synthetic mimic DNA (complementary match: target, single-base mismatch: 1MS, and double-base mismatch: 2MS) was added into the probe solution and measured at 10 min intervals for 2 h (F).

2.11. miRNA detection using lipoplex-composite hydrogels

The cylindrical hydrogels were incubated with 50 μL of a sample with TNaK buffer (1% of Triton X-100) for 2–3 h. Various concentrations (1 pM to 1 μM) of synthetic mimics, 250 ng of miRNAs extracted from the hippocampus, and 100 ng of plasma of the animal models were treated using the lipoplex-composite hydrogels. The fluorescence intensities were measured using the gel imaging system (Bio-Rad Laboratories, USA).

2.12. Method of manufacture of portable fluorometer

A portable fluorometer was constructed in-house in the laboratory. A light-emitting diode (LED) of wavelength 480 nm and a 486-nm bandpass filter (#65-085, Edmund Optics, Inc.) were employed to produce an excitation beam. The excitation beam was focused onto the sample using an aspheric condenser lens. The emission beam from the sample was filtered using 495-nm (FGL495S, Thorlabs Inc.) and 508-nm narrow band filters (#65-090, Edmund Optics, Inc.) to obtain the emission wavelength only. The filtered beam was detected using an Si diode (S2386-44K, Hammatsu), and the detected fluorescence signal was displayed on OLED using an Arduino Pro Mini.

2.13 miRNA detection using portable fluorometer

The cone-shaped hydrogels were transferred to a 1.5-mL microtube, with vertex facing the bottom, and incubated with 50 μL of a sample with TNaK buffer (1% of Triton X-100) for 2 h. Various concentrations (1 nM to 100 μM) of synthetic mimics were treated on the microtube. After incubation, the fluorescence intensities of the hydrogels were measured for 5 s (20 points) using the portable device.

2.14. Data analysis and statistics

Data were obtained via at least three independent experiments. The exact number of replicates is included in each graph. Data were reported as mean (m) ± SD. The following legends have been added to the figures: **p*-value < 0.05; ***p*-value < 0.005; and ****p*-value < 0.00005. Limit of detection (LOD) was calculated using the following equation: LOD = 3σ/m, where σ is the standard deviation of blank, and m is the slope of linear fitting of data in the linear range.

2.15. Collection and preparation of clinical samples for Alzheimer's disease

The clinical samples were prospectively obtained from Ajou University Medical Center from March 2019, under the approval of the ethical review (AJIRB-BMR-SMP-18-545). The study adhered to the principles of the Declaration of Helsinki and followed local clinical research regulations. All participants and their legal guardians (in cases of dementia) gave written informed consent. The clinical diagnosis of AD was based on the National Institute on Aging and Alzheimer's Association diagnostic guidelines (McKhann et al. 2011). ATN research framework was applied to clearly define Alzheimer's disease (AD; positive amyloid (A+), tau (T+) and neurodegeneration (N+) pathology) from non-AD (A-T-N-) control subjects based on neuroimaging (MRI and amyloid PET) and cerebrospinal fluid (CSF) biomarkers (the protein

concentration of Aβ42, phosphorylated tau at threonine 181 and total tau) (Jack et al. 2018). The measurements of CSF biomarkers and diagnostic cut-offs followed our previous literature (Park et al. 2017; Park et al. 2020). The pre-analytic handling method for plasma was previously described (Kim et al. 2015). Accordingly, AD (n = 8) and non-AD control (n = 8) were included for this study.

References

Elbert, D.L., Hubbell, J.A., 2001. Biomacromolecules 2, 430-441.

Jack, C. R., Jr., Bennett, D. A., Blennow, K., Carrillo, M. C., Dunn, B., Haeberlein, S. B., Holtzman, D. M., Jagust, W., Jessen, F., Karlawish, J., Liu, E., Molinuevo, J. L., Montine, T., Phelps, C., Rankin, K. P., Rowe, C. C., Scheltens, P., Siemers, E., Snyder, H. M., Sperling, R., 2018. Alzheimers Dement. 14, 535-562.

Kim, H. J., Park, K. W., Kim, T. E., Im, J. Y., Shin, H. S., Kim, S., Lee, D. H., Ye, B. S., Kim, J. H., Kim, E. J., Park, K. H., Han, H. J., Jeong, J. H., Choi, S. H., Park, S. A., 2015. J. Alzheimers Dis. 48, 1043-1050.

McKhann, G. M., Knopman, D. S., Chertkow, H., Hyman, B. T., Jack, C. R., Jr., Kawas, C. H., Klunk, W. E., Koroshetz, W. J., Manly, J. J., Mayeux, R., Mohs, R. C., Morris, J. C., Rossor, M. N., Scheltens, P., Carrillo, M. C., Thies, B., Weintraub, S., Phelps, C. H., 2011. Alzheimers Dement. 7, 263-269.

Park, S. A., Chae, W. S., Kim, H. J., Shin, H. S., Kim, S., Im, J. Y., Ahn, S. I., Min, K. D., Yim, S. J., Ye, B. S., Seo, S. W., Jeong, J. H., Park, K. W., Choi, S. H., Na, D. L., 2017. Alzheimer Dis. Assoc. Disord. 31, 13-18.

Park, S. A., Jung, J. M., Park, J. S., Lee, J. H., Park, B., Kim, H. J., Park, J. H., Chae, W. S., Jeong, J. H., Choi, S. H., Baek, J. H., 2020. Sci. Rep. 10 , 7423.

Stevens, K.R., Miller, J.S., Blakely, B.L., Chen, C.S., Bhatia, S.N., 2015. J. Biomed. Mater. Res. A 103, 3331-3338.

Zhang, H., 2017. Methods. Mol. Biol. 1522, 17-22.

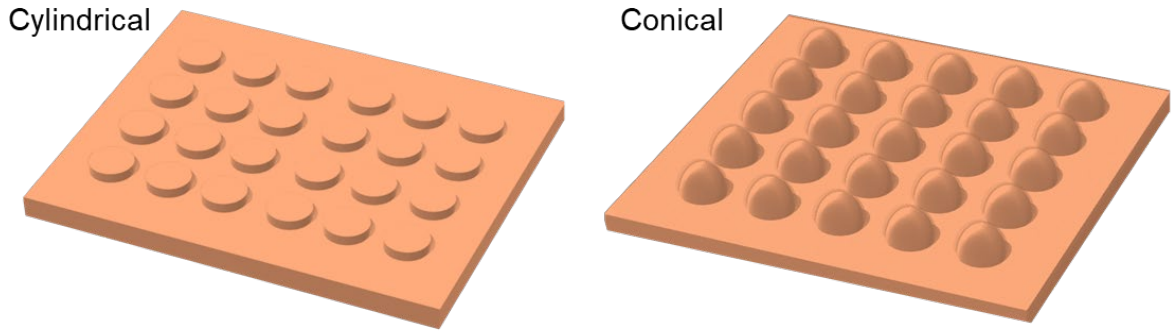

Figure S1. 3D structures for construction of hydrogel molds via soft lithography.

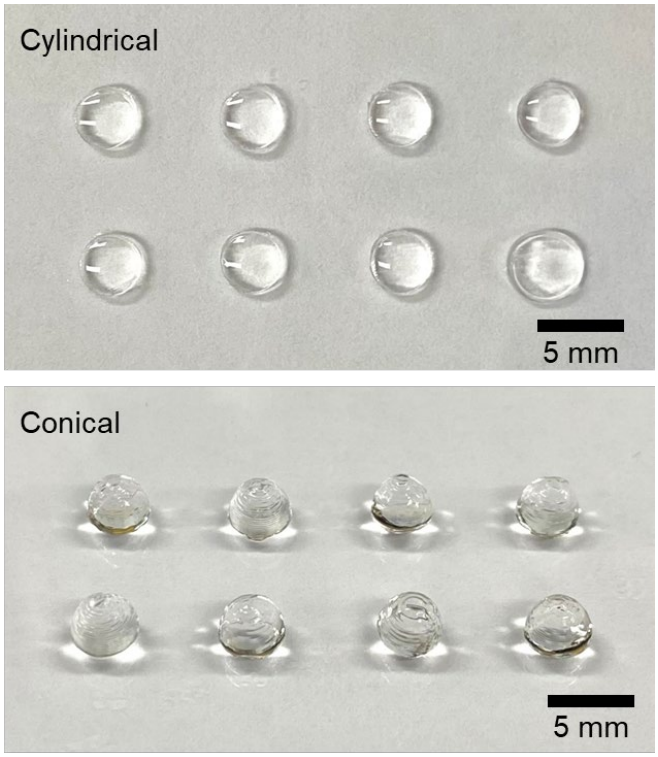

Figure S2. Images of cylindrical and conical hydrogels.

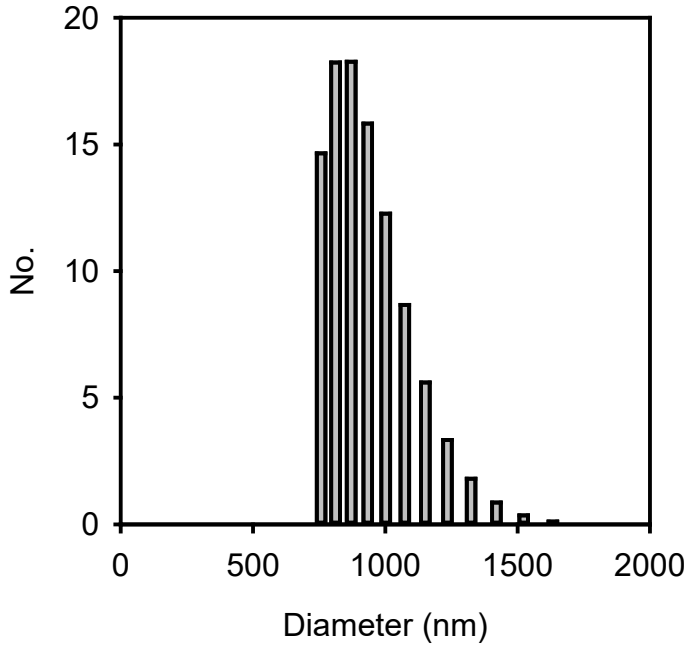

Figure S3. Size measurement of lipoplex nanoparticles (LNs).

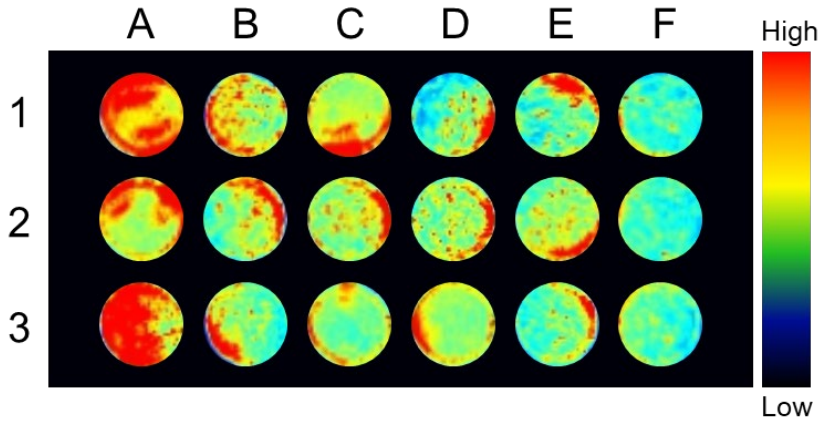

Figure S4. Fluorescence images of miR-sensing hydrogels with various concentrations of the target. A, 100 nM; B, 10 nM; C, 1 nM; D, 100 pM; E, 10 pM; F, Blank. The fluorescence of miR-sensing hydrogel measured from triplicate tests.

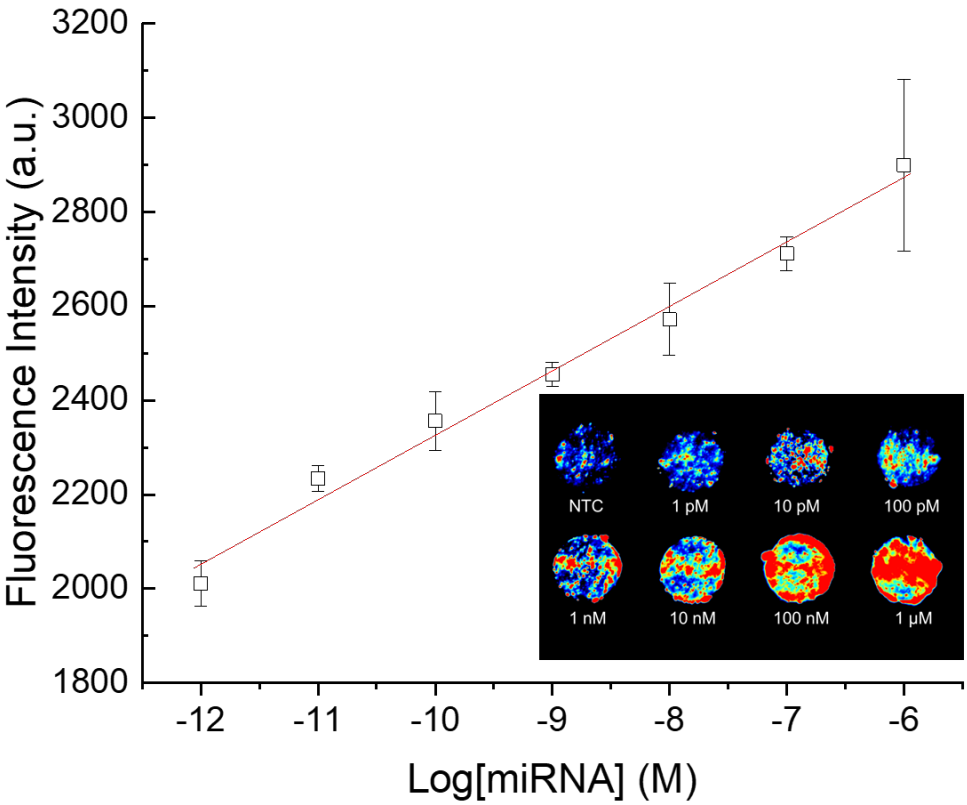

Figure S5. Sensitivity of lipoplex-composite hydrogel. Detection limits are estimated using various concentrations of target RNA (1 pM to 1 μM). The fluorescence of miR-sensing hydrogel measured from triplicate tests.

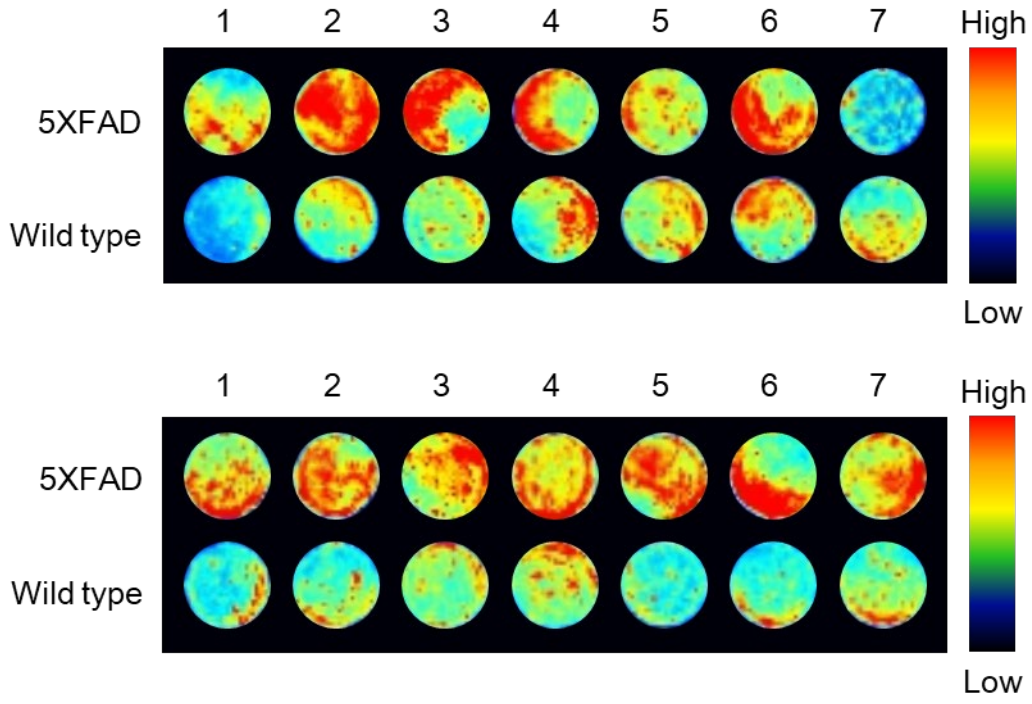

Figure S6. Fluorescence images of miR-sensing hydrogel with RNA sample that isolated from the hippocampus tissue (up) and plasma (down) (n = 7). Total of 250 ng of tissue RNAs and 100 ng of plasma RNAs were treated to miR-sensing hydrogels.

Table S1. Sequence information for probes used.

Name	Sequences of oligonucleotide (5′ to 3′)
H1	[FAM]tgt gtg tgt gag tgt ggg atc gaa agt gtg tgc aca ctc aca cac aca cac tca[BHQ1]
H2	tgt ggg atc gaa agt gtg tgt gtg tga gtg tgc aca cac ttt cga tcc cac act cac a
T*	tga gtg tgt gtg tgt gag tgt gt
1MS**	tga gtg tg***g*** gtg tgt gag tgt gt
2MS***	tga gt***c*** tg***g*** gtg tgt gag tgt gt

*T: Target gene sequence, **1MS: 1 base mismatched sequence, ***2MS: 2 base mismatched sequence
Italic: mismatched base, underline: stem of hairpin,

Supplementary Table 2. Microarray analysis of miRNA

Name	Fold change*	Regulation	Name	Fold change	Regulation
mmu-miR-1187	6.664192	Up	mmu-miR-6236	−2.014162	Down
mmu-miR-1306-3p	3.645584	Up	mmu-miR-325-5p	−2.025826	Down
mmu-miR-7038-3p	3.577297	Up	mmu-mir-335	−2.029494	Down
mmu-miR-5113	3.226746	Up	mmu-miR-7658-5p	−2.034452	Down
mmu-miR-669n	3.002366	Up	mmu-miR-370-5p	−2.037472	Down
mmu-miR-669c-5p	3.001534	Up	mmu-miR-1247-3p	−2.048986	Down
mmu-miR-365-2-5p	2.831114	Up	mmu-miR-376b-3p	−2.049966	Down
mmu-miR-3095-3p	2.790570	Up	mmu-miR-200a-3p	−2.060165	Down
mmu-miR-365-1-5p	2.733558	Up	mmu-miR-3474	−2.060165	Down
mmu-miR-1931	2.673000	Up	mmu-miR-1907	−2.070128	Down
mmu-miR-1306-5p	2.610724	Up	mmu-miR-5121	−2.070128	Down
mmu-miR-7001-5p	2.456459	Up	mmu-miR-7689-3p	−2.070128	Down
mmu-miR-23a-5p	2.379882	Up	mmu-miR-1981-3p	−2.075012	Down
mmu-miR-574-5p	2.257913	Up	mmu-miR-125b-2-3p	−2.092794	Down
mmu-mir-466j	2.243545	Up	mmu-miR-23b-5p	−2.100758	Down
mmu-miR-3061-5p	2.199842	Up	mmu-miR-1966-5p	−2.101748	Down
mmu-miR-8117	2.172686	Up	mmu-miR-344c-3p	−2.101748	Down
mmu-miR-15a-3p	2.169000	Up	mmu-mir-467b	−2.101763	Down
mmu-miR-665-5p	2.169000	Up	mmu-miR-381-5p	−2.150243	Down
mmu-miR-669m-5p	2.128283	Up	mmu-miR-6989-5p	−2.151153	Down
mmu-miR-466m-5p	2.128283	Up	mmu-miR-598-3p	−2.168609	Down
mmu-miR-668-5p	2.121493	Up	mmu-miR-1930-5p	−2.169	Down
mmu-mir-466j	2.105131	Up	mmu-miR-3962	−2.169000	Down
mmu-miR-6997-5p	2.034452	Up	mmu-miR-666-3p	−2.169827	Down
mmu-miR-7684-5p	2.012892	Up	mmu-miR-299a-3p	−2.172686	Down

mmu-miR-340-5p	−2.187708	Down	mmu-miR-3057-5p	−2.663051	Down
mmu-miR-467b-3p	−2.187708	Down	mmu-miR-3068-3p	−2.814308	Down
mmu-mir-666	−2.211124	Down	mmu-miR-1249-5p	−2.860208	Down
mmu-miR-7235-5p	−2.229809	Down	mmu-miR-1940	−2.863918	Down
mmu-miR-872-3p	−2.235194	Down	mmu-miR-503-5p	−2.914140	Down
mmu-miR-467d-3p	−2.242581	Down	mmu-miR-322-3p	−3.039871	Down
mmu-miR-7240-5p	−2.263805	Down	mmu-miR-3093-3p	−3.048501	Down
mmu-miR-6986-5p	−2.265485	Down	mmu-miR-140-5p	−3.055122	Down
mmu-miR-6981-5p	−2.311277	Down	mmu-miR-101b-3p	−3.211751	Down
mmu-miR-6988-3p	−2.345198	Down	mmu-miR-218-2-3p	−3.226746	Down
mmu-miR-19b-3p	−2.356752	Down	mmu-miR-1912-3p	−3.327365	Down
mmu-miR-592-3p	−2.366508	Down	mmu-miR-203-3p	−3.397727	Down
mmu-miR-3076-5p	−2.366508	Down	mmu-miR-322-5p	−3.693478	Down
mmu-miR-3093-5p	−2.456459	Down	mmu-miR-501-5p	−3.757857	Down
mmu-miR-6360	−2.456459	Down	mmu-miR-154-3p	−3.865915	Down
mmu-miR-383-3p	−2.492131	Down	mmu-miR-222-5p	−3.883022	Down
mmu-miR-496a-3p	−2.532654	Down	mmu-miR-551b-5p	−4.043039	Down
mmu-miR-5129-3p	−2.532654	Down	mmu-miR-25-5p	−4.061746	Down
mmu-miR-467a-5p	−2.541200	Down	mmu-miR-200c-3p	−4.087390	Down
mmu-miR-410-3p	−2.618517	Down	mmu-miR-301a-3p	−4.979980	Down
mmu-miR-3068-5p	−2.626861	Down	mmu-miR-744-3p	−5.227133	Down
mmu-miR-539-5p	−2.636602	Down	mmu-miR-3107-3p	−5.710235	Down
mmu-miR-362-3p	−2.661482	Down			

* cut off; fold-change Log_2 (5XFAD/WT) ≥ 2.0

Supplementary Table 3.

Transcript ID	Fold change	miR-sequence	Transcript ID	miR-sequence	100% agreement
mmu-miR-1187	6.66	UAUGUGUGUGUGUAUGUGUGUAA			
mmu-miR-1306-3p	3.65	ACGUUGGCUCUGGUGGUGAUG	hsa-miR-1306-3p	ACGUUGGCUCUGGUGGUG	
mmu-miR-7038-3p	3.58	CACUGCUCCUGCCUUCUUACAG			
mmu-miR-5113	3.23	ACAGAGGAGGAGAGAGAUCCUGU			
mmu-miR-669n	3.00	AUUUGUGUGUGGAUGUGUGU			
mmu-miR-669c-5p	3.00	AUAGUUGUGUGUGGAUGUGUGU			
mmu-miR-365-2-5p	2.83	AGGGACUUUCAGGGGCAGCUGUG	hsa-miR-365b-5p	AGGGACUUUCAGGGGCAGCUGU	
mmu-miR-3095-3p	2.79	AAGCUUUCUCAUCUGUGACACU			
mmu-miR-365-1-5p	2.73	AGGGACUUUUGGGGGCAGAUGUG	hsa-miR-365a-5p	AGGGACUUUUGGGGGCAGAUGUG	√
mmu-miR-1931	2.67	AUGCAAGGGCUGGUGCGAUGGC			
mmu-miR-1306-5p	2.61	CACCACCUCCCCUGCAAACGUCC	hsa-miR-1306-5p	CCACCUCCCCUGCAAACGUCCA	
mmu-miR-7001-5p	2.46	AGGCAGGGUGUGAGCGUGAGCAU			
mmu-miR-23a-5p	2.38	GGGGUUCCUGGGGAUGGGAUUU	hsa-miR-23a-5p	GGGGUUCCUGGGGAUGGGAUUU	√
mmu-miR-574-5p	2.26	UGAGUGUGUGUGUGUGAGUGUGU	hsa-miR-574-5p	UGAGUGUGUGUGUGUGAGUGUGU	√
mmu-mir-466j	2.24	CAGUGGGCCGUGAAAGGUAGCC			
mmu-miR-3061-5p	2.20	GCUCGUGUGGAACAGAAGGGG			
mmu-miR-8117	2.17	CAGGCCAUA*C*UGUGCUGCCUCA	hsa-miR-15a-3p	CAGGCCAUAUUGUGCUGCCUCA	
mmu-miR-15a-3p	2.17	AGGGGCCUCUGCCUCUAUCCAGGAUU	hsa-miR-665	ACCAGGAGGCUGAGGCCCCU	
mmu-miR-665-5p	2.17	UGUGUGCAUGUGCAUGUGUGUAU			
mmu-miR-669m-5p	2.13	UGUGUGCAUGUGCAUGUGUGUAU			
mmu-miR-466m-5p	2.13	GUAAGUGUGCCUCGGGUGAGCAUG	hsa-miR-668-5p	UGCGCCUCGGGUGAGCAUG	
mmu-miR-668-5p	2.12	UAACAGGCUGGAGAGGUGCAGA			
mmu-mir-466j	2.11	UCUGGGAAGCCUGGGCAGCAG			
mmu-miR-6997-5p	2.03	UAUGUGUGUGUGUAUGUGUGUAA			
mmu-miR-7684-5p	2.01	ACGUUGGCUCUGGUGGUGAUG	hsa-miR-1306-3p	ACGUUGGCUCUGGUGGUG	